AGU PUBLICATIONS

Geophysical Research Letters

RESEARCH LETTER
10.1002/2017GL076592

Key Points:
- We model the effects of marine sedimentary water storage on sea-level changes driven by global sediment redistribution
- Sedimentary water storage driven by modern sediment fluxes can have meter-scale effects on global mean sea level over 10^5 year timescales
- This illustrates the importance of accounting for sedimentary water storage in modeling long-term sea-level change

Supporting Information:
- Supporting Information S1
- Data Set S1

Correspondence to:
K. L. Ferrier,
ferrier@gatech.edu

Citation:
Ferrier, K. L., Li, Q., Pico, T., & Austermann, J. (2018). The influence of water storage in marine sediment on sea-level change. *Geophysical Research Letters*, *45*. https://doi.org/10.1002/2017GL076592

Received 28 NOV 2017
Accepted 19 FEB 2018
Accepted article online 28 FEB 2018

The Influence of Water Storage in Marine Sediment on Sea-Level Change

Ken L. Ferrier[1], Qi Li[1], Tamara Pico[2], and Jacqueline Austermann[3]

[1]School of Earth and Atmospheric Sciences, Georgia Institute of Technology, Atlanta, GA, USA, [2]Department of Earth and Planetary Sciences, Harvard University, Cambridge, MA, USA, [3]Department of Earth Sciences, University of Cambridge, Cambridge, UK

Abstract Sea-level changes are of wide interest because they provide information about Earth's internal structure and the sensitivity of ice sheets to climate change. Here we illustrate the sensitivity of sea level to marine sedimentary water storage by modeling sea-level responses to a synthetic global sediment redistribution history in which rates and patterns of erosion and deposition are similar to those at present and steady in time from the Last Interglacial to present. Our simulations show that if sediment redistribution were accounted for but sedimentary water storage were neglected, modeled sea-level changes could be overestimated by ~2 ± 1 m of global mean sea-level equivalent, a significant fraction of published estimates of 6–9 m of global mean sea-level change since the Last Interglacial. These results show that sedimentary water storage may significantly contribute to changes in Earth's long-term seawater budget over $>10^5$ year timescales and underscore the importance of accounting for it in modeling long-term sea-level changes.

Plain Language Summary Sea-level changes are of wide interest because they reflect changes in climate and affect coastal flooding hazards. Recent advances in sea-level modeling now make it possible to compute how sea-level changes are affected by the storage of water in the pore space of seafloor sediment, an effect that had not been included in previous models. To illustrate this effect, this study computes sea-level responses to simulated global erosion and deposition histories over a single ice-age cycle, from the Last Interglacial (~120,000 years ago) to the present. These simulations show that if sea-level models accounted for sediment deposition but neglected water storage in seafloor sediment, modeled sea-level changes since the Last Interglacial could be overestimated by the globally averaged equivalent of about 2 ± 1 m. This is a significant fraction of published estimates of globally averaged sea-level change (6–9 m) since the Last Interglacial. These results imply that water storage in sediment can significantly affect Earth's seawater volume over geologic time and demonstrate the importance of accounting for this effect in modeling long-term sea-level changes.

1. Introduction

1.1. Effects of Sediment Redistribution on Sea-Level Change

Changes in sea level are of wide interest because they influence coastal flooding hazards (Woodruff et al., 2013), provide insight into Earth's viscoelastic structure (e.g., Cathles, 1975; Paulson et al., 2007), and reflect the sensitivity of ice sheets to climate change (e.g., Dutton & Lambeck, 2012; Kopp et al., 2009, 2013). Because changes in ice loading, dynamic topography, Earth rotation, and sediment redistribution all induce local sea-level changes, interpretations of global mean sea-level changes must be interpreted in light of all these processes. These considerations have motivated the continued refinement of gravitationally self-consistent sea-level models, which, since the classic study of Farrell and Clark (1976), have included extensions to account for shoreline migration (Johnston, 1993; Milne, 1998; Milne et al., 1999; Peltier, 1994), Earth rotation (Milne & Mitrovica, 1996, 1998), 3-D variations in Earth structure (Latychev et al., 2005; Martinec, 2000; Wu & van der Wal, 2003; Zhong et al., 2003), dynamic topography (Austermann & Mitrovica, 2015), and sediment redistribution (Dalca et al., 2013; Ferrier et al., 2017).

Sediment redistribution can generate sea-level changes in several ways. The primary effect of sediment deposition is to directly change local sea level by modifying the elevation of the solid surface, which is the sum of the crustal elevation, grounded ice thickness, and sediment thickness (Dalca et al., 2013), and which therefore increases during deposition and decreases during crustal subsidence and sediment compaction. Because newly deposited marine sediment occupies space that had previously been occupied by water, deposition induces a redistribution of seawater and an increase in the global mean sea surface elevation (Conrad, 2013; Harrison, 1990, 1999; Harrison et al., 1981; Miller et al., 2005; Müller et al., 2008; Southam & Hay, 1977). Over long timescales, these effects can be large. Temporal variations in deposition rates over the Cenozoic, for example, have been estimated to be responsible for increasing sea level by 60 ± 20 m (Conrad, 2013).

A second effect of deposition is on the gravitational equipotential surface that sets the sea surface elevation. Sediment deposition modifies the surface load and the gravity field, with large deposits drawing water toward them and locally increasing the sea surface elevation (Dalca et al., 2013). Recent studies in the Mississippi, Indus, and Yellow River systems suggest that perturbations in the elevation of the sea surface equipotential are small but nonnegligible, with amplitudes reaching ~5% of the magnitude of crustal deformation induced by sediment loading (Ferrier et al., 2015; Pico et al., 2016; Wolstencroft et al., 2014).

A third effect is the incorporation of water into the pore space of deposited sediment, which reduces the volume of water displaced by sediment (Southam & Hay, 1981). The effects of continental groundwater storage on sea level have been examined in a number of studies (e.g., Ingebritsen & Manning, 2002; Veit & Conrad, 2016; Wada et al., 2010), but the effects of water storage in marine sediment, while widely recognized, have only recently been incorporated into gravitationally self-consistent sea-level models (Ferrier et al., 2017). For this reason it is not well known how sedimentary water storage affects sea-level changes or how those changes are spatially distributed. The net effect of sediment redistribution can be locally significant over sufficiently long timescales, with sea-level perturbations near the outlets of large rivers exceeding 100 m over a single ~120 kyr glacial cycle (Ferrier et al., 2015; Kuchar et al., 2017; Pico et al., 2016; Wolstencroft et al., 2014).

1.2. The Magnitude of Marine Sedimentary Water Storage

A rough calculation suggests that changes in marine sedimentary water storage may be a significant component of sea-level changes over the ~10^5 year timescales between interglacials. Global surveys of sedimentary deposits imply a global land-to-ocean sediment flux of ~21 Gt year^{-1} (Wilkinson & McElroy, 2007). If marine sedimentary water storage were neglected, this flux combined with a mean sediment deposit density of 1,500 kg m^{-3} (e.g., Brain et al., 2012) would imply a displacement of ~$1.4 \cdot 10^{15}$ m^3 of water over the ~10^5 year timespan between interglacials, equivalent to ~4.5 m of global mean sea level (GMSL). Field measurements show that marine sediments gradually compact after being deposited with a high porosity (50–90%), such that a sediment column several kilometers thick retains a vertically averaged mean porosity of ~20–40% after compaction (e.g., Bahr et al., 2001; Goldobin, 2011; Mondol et al., 2007; Spinelli et al., 2004; Spinelli & Underwood, 2004). This implies a significant influx of water into deposited sediment, and a commensurately smaller displacement of water by the deposited sediment. A mean porosity of 20–40%, for instance, would imply a net flux of water of ~$3\text{–}6 \cdot 10^{14}$ m^3 into marine sediment over 10^5 years, or a net removal of water from the oceans equivalent to ~1–2 m GMSL. Both this water trapped in sediment and the remaining ~2.5–3.5 m of water displaced by sediment are significant relative to estimates of GMSL at the Last Interglacial (LIG) at ~130–115 ka (>6.6 m above modern GMSL at 95% confidence; Kopp et al., 2009, 2013; 6–9 m above modern GMSL; Dutton & Lambeck, 2012). Note that this rough calculation neglects subsidence of the ocean crust under sediment as well as gravitational or deformational effects and that including these effects in rigorous sea-level simulations is the purpose of this study.

The rough calculation in the preceding paragraph suggests that sedimentary water storage may also be a significant component of Earth's long-term seawater budget. The volume flux of water into sediment calculated above corresponds to a mass flux of $3\text{–}6 \cdot 10^{12}$ kg year^{-1}, larger than rates of seawater loss by subduction ($74\text{–}288 \cdot 10^{10}$ kg year^{-1}; Bebout, 1995; Wallmann, 2001; Jarrard, 2003; Parai & Mukhopadhyay, 2012) and seawater gain by volcanism ($21\text{–}174 \cdot 10^{10}$ kg year^{-1}; Bounama et al., 2001; Fischer, 2008; Hilton et al., 2002; Ito et al., 1983; Shinohara, 2013).

The magnitude of these effects motivates a detailed study of the effects of sedimentary water storage on sea-level changes and the global water budget. That is our goal here. In this study, we apply the gravitationally self-consistent sea-level model in Ferrier et al. (2017) to quantify the sensitivity of sea-level changes—both in magnitude and spatial pattern—to marine sedimentary water storage. Our simulations show that marine sedimentary water storage can significantly affect sea level and the ocean water balance over 10^5 year timescales and therefore can affect interpretations of paleo-ice volumes at the LIG if sediment redistribution were accounted for but sedimentary water storage were neglected.

2. Modeling Sea-Level Responses to Global Sediment Redistribution

2.1. Model Overview

To quantify the effects of marine sedimentary water storage on sea level, we apply the gravitationally self-consistent sea-level model in Ferrier et al. (2017), to which we refer the reader for model details. This model computes temporal changes in sea level, ΔSL, by computing elevation changes in the sea surface equipotential (ΔG) and the crustal surface (ΔR) under applied changes in the thickness of grounded ice (ΔI) and sediment (ΔH).

$$\Delta SL = \Delta G - \Delta R - \Delta I - \Delta H \tag{1}$$

In this model, sediment is deposited with an initial porosity $\phi_{\max}$ and compacts at a rate proportional to the difference between the lithostatic and hydrostatic stresses (Table S2). Water is incorporated into sedimentary pore space and affects the global water balance (equation (2)), in which changes in ocean water volume are balanced by changes in ice volume and water storage in sediment (Ferrier et al., 2017).

$$\iint_\Omega \Delta S_j \, d\Omega = -\frac{\rho_I}{\rho_w} \iint_\Omega \Delta I_j \, d\Omega - \iint_\Omega \left(\overline{\phi}_j f_{wj} H_j - \overline{\phi}_0 f_{w0} H_0 \right) d\Omega \tag{2}$$

Here the double integral over Ω is an integral over the Earth's surface; ΔS_j and ΔI_j are the changes in the thicknesses of ocean water and grounded ice from t_j to t_0, respectively; H_j and H_0 are the thicknesses of sediment at t_j and t_0, respectively; $\overline{\phi}_j$ and $\overline{\phi}_0$ are the vertically-averaged mean porosity of the sediment column at t_j and t_0, respectively; f_{wj} and f_{w0} are the fraction of the sedimentary pore space in the sediment column that is filled with water at t_j and t_0, respectively; and ρ_w and ρ_I are the densities of water and ice, respectively.

2.2. Model Inputs

We apply this model to rigorously quantify the effect of marine sedimentary water storage on changes in sea level, and use the time from the LIG (~122 ka) to the present as an illustrative case study. Because our goal is to isolate the sensitivity of sea-level changes to marine sedimentary water storage, in these simulations we maintain a temporally constant ice distribution equal to that at present in ICE-5G (Peltier, 2004) and drive the sea-level model with only sediment redistribution histories. For this reason, the resulting simulations should not be considered representations of the true sea-level history over the last glacial period; instead, they should be considered simulations aimed at isolating the sensitivity of sea-level changes to marine sedimentary water storage.

We constructed two global sediment transfer scenarios to quantify the sensitivity of sea-level responses to marine sedimentary water storage. These sediment transfer scenarios are constrained to have a total land-to-ocean sediment flux of 20 Gt year^{-1}, comparable to the measured global flux (Wilkinson & McElroy, 2007), and are assigned spatial and temporal variations in erosion and deposition rates that are intentionally highly simplified relative to the true variations. This approach is useful for isolating the sensitivity of modeled sea-level changes to sedimentary water storage, because, as we show below, the effects of marine sedimentary water storage are primarily sensitive to the magnitude of the global sediment flux and are relatively insensitive to spatial and temporal variations in sediment redistribution. We emphasize that this approach is valid only for isolating the effects of sedimentary water storage and that accurately modeling sea-level responses to sediment redistribution everywhere on Earth would require accounting for the complex spatial and temporal variations in erosion and deposition across the planet (e.g., Ferrier et al., 2015; Pico et al., 2016; Wolstencroft et al., 2014).

The first scenario (Scenario A) is designed to account for the effects of sedimentary water storage. This is the standard scenario against which we compare other simulations. Here we use the global fluvial flux compilation of Milliman and Farnsworth (2011) to assign erosion rates to all river basins with a mass flux F_b of at least 10 Mt/year (n = 105), using predam fluxes for rivers with reported predam fluxes. Geographic extents for these basins were taken from U.S. Geological Survey HydroSHEDS, GRDC, and Watersheds of the World databases (Global Runoff Data Centre, 2007; Lehner et al., 2006; Revenga et al., 1998) and resampled to a global grid of 512 latitudinal by 1,024 longitudinal grid points. Erosion rates were assigned to be spatially invariant

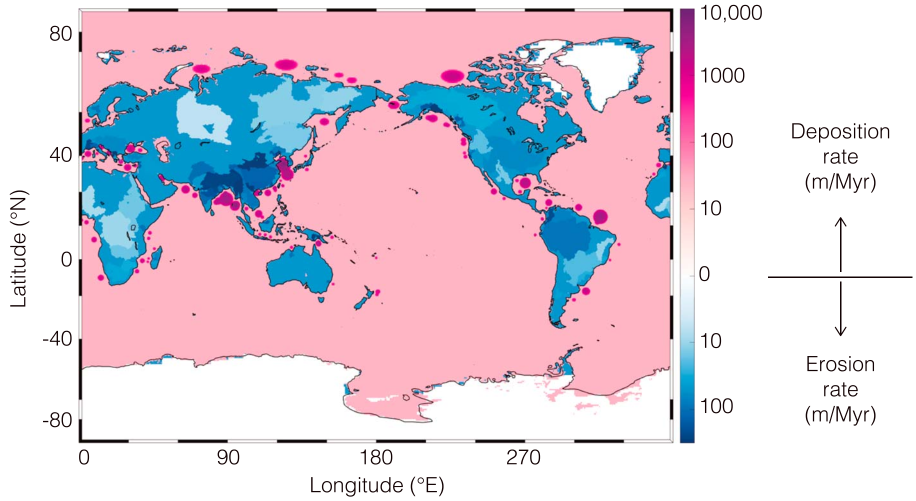

Figure 1. Erosion rates (blue) and deposition rates (red) used to create the sediment redistribution Scenarios A and B.

within each basin and scaled such that the sediment flux from each basin equaled the river's modern sediment flux for an eroded bedrock density of ρ_s = 2650 kg m^{-3} (Table S1). These 105 drainage basins have a total mass flux of 10.56 Gt/year, or 53% of the global flux of 20 Gt/year adopted in this simulation (Wilkinson & McElroy, 2007). Erosion rates in regions with grounded ice were set to zero. Subaerial regions outside the mapped basins and grounded ice were delineated as those above modern sea level using ETOPO2 (United States Department of Commerce National Oceanic and Atmospheric Administration National Geophysical Data Center, 2001) and assigned a spatially uniform erosion rate of 47.55 m/Myr, such that the globally integrated land-to-ocean sediment flux totaled 20 Gt/year. To highlight the role of water storage in marine sediment, we neglect changes in continental groundwater storage by assigning the eroded sediment to be dry (i.e., $\overline{\phi}$ = 0 and f_w = 0 in equation (2)).

To ensure that sediment mass is conserved between the eroded and deposited sediment, we generated a marine deposit near each basin's outlet with the same integrated sediment mass accumulation rate as the basin's mass flux. Deposition rates in each basin's deposit were modeled as a paraboloid with a circular base and a vertically parabolic cross section, the locations of which are given in Table S1. This sediment was deposited atop the local seafloor topography given by ETOPO2 (United States Department of Commerce National Oceanic and Atmospheric Administration National Geophysical Data Center, 2001), such that the seafloor topography within these deposits was continually modified by a paraboloidal sediment deposition rate and sediment compaction. The angular radius $r_{angular}$ of each deposit's base was computed as $r_{angular} = a(F_b)^{1/3}$ with a = 0.004 °/(t year^{-1})$^{1/3}$, such that a fluvial mass flux of 10^9 t year^{-1} (comparable to that in the largest rivers; Table S1) would generate a deposit with a basal radius of 4°. The deposition rate at the center of the deposit was calculated as $B_{center} = 2F_b(\pi r^2 \rho_s(1 - \phi_{max}))^{-1}$, where r is the linear radius of the deposit base. Deposition rates elsewhere in the deposit decrease parabolically with distance d from the center of the deposit as $B = B_{center}(1 - d^2/r^2)$. Deposits generated in this manner that were too wide for the locally available seafloor were laterally truncated by the shoreline and rescaled to ensure that the deposit occupied only oceanic grid cells and that the deposit's sediment mass accumulation rate matched the associated basin's mass flux. Aside from constraining the synthetic deposits to lie entirely on the seafloor, the deposits were constructed independently of the local seafloor bathymetry. After generating deposits for each river, we assigned a spatially uniform deposition rate of 25.17 m/Myr to the remainder of the seafloor such that the globally integrated deposition rate equaled the globally integrated erosion rate (20 Gt/year). To focus on the role of water storage in marine sediment, we assigned full saturation to marine sediment (i.e., f_w = 1).

We used the resulting map of erosion and deposition rates (Figure 1) to construct a sediment transfer scenario over the past 122 kyr. Erosion rates and deposition rates were held constant in time during the simulation. Following Ferrier et al. (2017), sediment is deposited with an initial porosity of ϕ_{max} = 0.6, and sediment thickness, bulk sediment density, and sedimentary water storage evolve over time under deposition and compaction (Table S2).

The second scenario (Scenario B) is designed to neglect marine sedimentary water storage but to be otherwise as similar as possible to Scenario A. Scenario B is assigned the same spatial and temporal patterns in sediment thickness and vertically averaged sediment density $\overline{\rho}_H$ as Scenario A, which ensures that changes in the sediment load are identical in Scenarios A and B. Unlike Scenario A, Scenario B is assigned a porosity of zero in the deposited sediment to ensure that no water is stored in the sediment deposits, which mimics the behavior of previous models that did not account for sedimentary water storage (Dalca et al., 2013). The critical difference between Scenarios A and B is that the load in the marine deposits in Scenario A is due to a mixture of sediment particles and water-filled pore space, while in Scenario B it is due to sediment alone. This permits us to isolate the effect of water storage on ΔSL without introducing the potentially complicating effects of differences in loading from the sediment deposits. In both Scenarios A and B, sediments are deposited atop impermeable crust that does not contribute to the global water balance.

We computed responses to these sediment redistribution scenarios using a spherically symmetric Earth model with elasticity and density profiles given by the Preliminary Reference Earth Model (Dziewonski & Anderson, 1981), modern topographic data given by ETOPO2 (United States Department of Commerce National Oceanic and Atmospheric Administration National Geophysical Data Center, 2001), and a radial viscosity profile known as VM2 with an elastic lithosphere that is 90 km thick (Peltier, 2004). Because marine sedimentary water storage is primarily sensitive to the global sediment flux and sediment porosity—factors that are independent of the Earth model—the effects of sedimentary water storage on sea level are largely insensitive to the choice of Earth model. Thus, in the following analysis, we illustrate the effects of sedimentary water storage using a single Earth model.

3. Results

Figures 2a–2c show ΔSL, ΔG, and ΔR at the end of the 122 kyr simulation in Scenario A, which we term ΔSL_{A}, ΔG_{A}, and ΔR_{A}, respectively. Figures 2d–2f show ΔSL, ΔG, and ΔR at the end of the 122 kyr simulation in Scenario B and are termed ΔSL_{B}, ΔG_{B}, and ΔR_{B}, respectively. Figures 2g–2i show the differences in these quantities between Scenarios A and B and are the errors associated with neglecting marine sedimentary water storage. We term these differences $\Delta SL_{\mathrm{B\text{-}A}}$, $\Delta G_{\mathrm{B\text{-}A}}$, and $\Delta R_{\mathrm{B\text{-}A}}$, respectively.

4. Discussion

4.1. Implications for Modeled Sea-Level Changes

Figure 2g shows that neglecting marine sedimentary water storage produces values of ΔSL that are higher everywhere than they would be if sedimentary water storage was accounted for. These errors, $\Delta SL_{\mathrm{B\text{-}A}}$, have a mean of 2.13 m over oceans and 1.61 m over land. The positive values indicate that neglecting sedimentary water storage produces modeled changes in ΔSL that are higher than they should be.

Superimposed on this nearly bimodal pattern are secondary patterns around coastlines. In the ocean ~400 km west of the coast of British Columbia, for instance, $\Delta SL_{\mathrm{B\text{-}A}}$ is as large as 2.21 m, about 4% larger than the average $\Delta SL_{\mathrm{B\text{-}A}}$ over the oceans. Mirroring this pattern on land, $\Delta SL_{\mathrm{B\text{-}A}}$ is as small as 1.51 m approximately 400 km inland of the same coast, about 3% smaller than $\Delta SL_{\mathrm{B\text{-}A}}$ in the North American interior. This is the signature of continental levering (Mitrovica & Milne, 2002), in which changes in loading on the ocean lithosphere induce uplift and subsidence on either side of coastlines due to the migration of the mantle under the oceanic and continental lithosphere. After the roughly bimodal difference between land and oceans, this continental levering signal is the largest spatially variable component in $\Delta SL_{\mathrm{B\text{-}A}}$.

Figures 2h and 2i show that the errors in ΔSL stem from two sources. First, in Scenario B, the constraint $\overline{\phi} = 0$ prevents water from being stored in the sediment deposit, such that all seawater is forced to lie above the deposit. This contrasts with Scenario A, where some water is stored in the deposit. Because the deposit thickness is constrained to be identical in each scenario, this results in a larger combined thickness of the deposit and overlying water—and thus a higher sea surface equipotential—in Scenario B ($\Delta G_{\mathrm{B}} > \Delta G_{\mathrm{A}}$). This error in ΔG averages 1.97 m and varies from 1.86 to 2.07 m across the Earth's surface in a pattern that reflects rotational effects on the sea surface (Milne & Mitrovica, 1996, 1998). This error in ΔG is the largest source of error in ΔSL.

The second source of error in ΔSL stems from the error in the combined load of water and sediment on the ocean crust, which is larger in Scenario B than in Scenario A. This occurs because the globally averaged

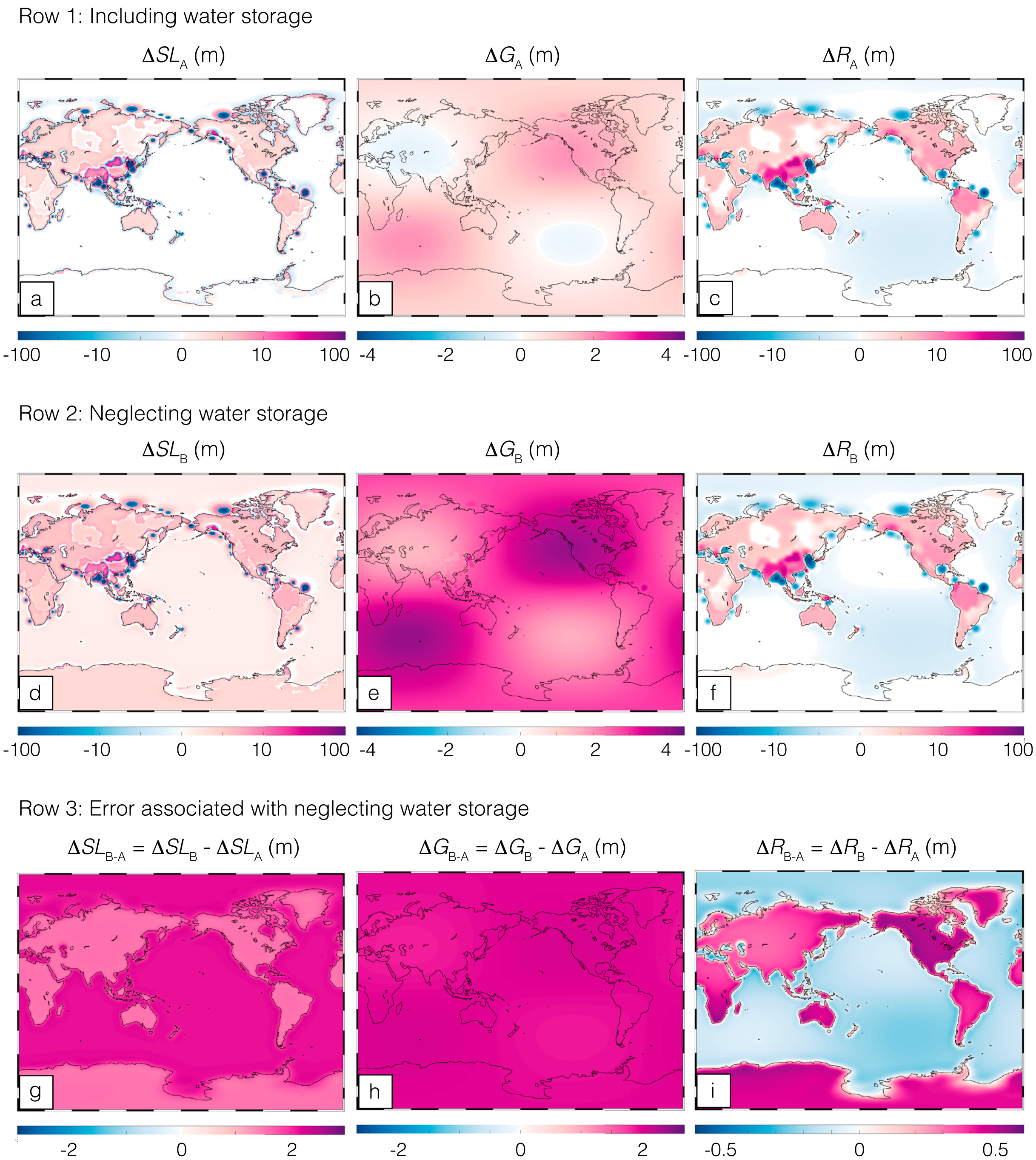

Figure 2. Effects of marine sedimentary water storage on modeled sea-level changes. (a–c) ΔSL, ΔG, and ΔR, respectively, at the end of a 122 kyr simulation driven by Scenario A, which accounts for sedimentary water storage. (d–f) ΔSL, ΔG, and ΔR, respectively, at the end of a 122 kyr simulation driven by Scenario B, which neglects sedimentary water storage but is otherwise identical to Scenario A. (g–i) The differences between these scenarios in ΔSL, ΔG, and ΔR, respectively, are the errors introduced by neglecting marine sedimentary water storage in Scenario B. Note that the color scheme in panels a, c, d, and f varies logarithmically.

change in the overlying water thickness is −2.13 m in Scenario A (Figure 2a) and zero in Scenario B (Figure 2d), while changes in the deposit load ($\overline{\rho}_H \Delta H$) are identical in Scenarios A and B. This produces in Scenario B a larger downward deflection of the ocean crust (i.e., a larger negative ΔR in the oceans), which in turn generates a larger upward deflection of the continental crust (i.e., a larger positive ΔR on land). This is also the source of the continental levering signal. This error in ΔR averages −0.15 m over the oceans and 0.36 m over land, or 7–18% of the magnitude of the average error in ΔG in Scenario B.

4.2. Implications for the Global Water Budget and Inferences of Paleo-Ice Volume

A by-product of the incorporation of water into marine sediment is the reduction in the volume of free ocean water. This has implications for modeling Earth's long-term seawater budget. The magnitude of this effect can be illustrated by applying the global water balance (equation (2)) to Scenario A. Here the simulation has been driven only by sediment redistribution, such that there are no changes in the water budget from changes in ice. Despite the absence of changes in ice volume, however, changes in ocean water volume are not zero. The integrated change in ocean water volume at the end of the simulation is $-7.7 \cdot 10^{14}$ m^3, or -2.1 m GMSL.

This flux of $7.7 \cdot 10^{14}$ m^3 over the 122 kyr simulation translates to a water flux into sediment of ~$630 \cdot 10^{10}$ kg/year. This is ~4–30 times larger than published estimates of water fluxes into the ocean from volcanism ($21–174 \cdot 10^{10}$ kg/year; Ito et al., 1983; Bounama et al., 2001; Hilton et al., 2002; Fischer, 2008; Shinohara, 2013) and ~2–8 times larger than water fluxes into the mantle by subduction ($74–288 \cdot 10^{10}$ kg/year; von Huene & Scholl, 1991; Parai & Mukhopadhyay, 2012). We do not explore these additional water mass fluxes in this study, nor the expulsion of water from sediments in accretionary prisms (Moore & Vrolijk, 1992; Screaton et al., 2002; Spinelli et al., 2004; Spinelli & Underwood, 2004; von Huene & Scholl, 1991), although we note that the sea-level model is general enough to accommodate such processes in future studies. While there are substantial uncertainties on all these fluxes, the rate of water incorporation into sediments relative to these processes implies that a complete seawater budget over ~10^5 year timescales must account for changes in sedimentary water storage. The potential magnitude of these effects serves as motivation for collecting further measurements of water fluxes into and out of sediments, especially over long timescales.

These simulations have implications for inferences of changes in paleo-ice volume drawn from modeled changes in sea level. An illustrative example of this is given by Scenario A. Since changes in sedimentary water storage are not negligible in this scenario, they need to be accounted for when inferring ice volume change from changes in the global water budget, as in equation (2) ($\iint_\Omega \Delta I_j d\Omega = -(\rho_w/\rho_I)\iint_\Omega \Delta S_j d\Omega - (\rho_w/\rho_I) \iint_\Omega \left(\overline{\phi}_j f_{wj} H_j - \overline{\phi}_0 f_{w0} H_0\right) d\Omega$). Applying this expression to Scenario A would result in an inference of no change in global ice volume, as expected for a simulation with a temporally constant ice distribution. If, however, the change in ice volume had been inferred only from the change in ocean water volume (i.e., $\iint_\Omega \Delta I_j d\Omega = -(\rho_w/\rho_I)\iint_\Omega \Delta S_j d\Omega$), as is common in models that neglect sedimentary water storage (e.g., Dalca et al., 2013), this would have led to the incorrect inference that global ice volume had increased by ~2 m GMSL over the duration of the simulation. An error of this magnitude would be significant in the context of published estimates of 6–9 m GMSL changes from LIG to present based on elevation differences between LIG paleoshorelines and modern shorelines (Dutton & Lambeck, 2012; Kopp et al., 2009, 2013). While these studies do not include the effect of sediment redistribution, we show here that simulations that do account for sediment redistribution but neglect water storage would overestimate the change in ice volume since the LIG by ~2 m GMSL. Such simulations would mistakenly attribute modeled changes in ocean water volume only to changes in ice volume, rather than partly to water fluxes into sediment and partly to changes in ice volume. We stress that the size of such an error would depend on the magnitude of the global sediment flux and sedimentary pore volume and therefore would be subject to uncertainties in both of these quantities, as described below.

4.3. Uncertainties in the Effects of Sedimentary Water Storage

The primary uncertainty in the effects of marine sedimentary water storage on ΔSL is the uncertainty in the magnitude of the global sediment flux. Estimates of modern global sediment fluxes range from 8.3 to 51.1 Gt/year (mean and standard deviation of these estimates: 18 ± 9 Gt/year; Willenbring et al., 2013). Since the modeled water volume stored in marine sediment depends approximately linearly on the global sediment flux for a given geometry of deposition (Figure S1), uncertainties in the effects of sedimentary water storage should scale roughly linearly with uncertainties in the global sediment flux. To the extent that the ~50% standard deviation in published global sediment fluxes reflects uncertainties in the true global sediment flux, this suggests that marine sedimentary water storage in Scenario A should be ~2 ± 1 m. This lends importance to accurately quantifying past and present global sediment fluxes (e.g., Kirchner & Ferrier, 2013; Larsen et al., 2014; Wilkinson & McElroy, 2007; Willenbring et al., 2013).

A secondary control on the effects of sedimentary water storage on ΔSL is the spatial pattern of sediment redistribution. Globally, there are large uncertainties in the spatial distribution of deposition and erosion (e.g., Syvitski et al., 2005). These uncertainties, however, translate to relatively small uncertainties in the effects of sedimentary water storage on GMSL, because the errors associated with neglecting sedimentary water storage are primarily sensitive to the total volume of deposited sediment, and only secondarily sensitive to how it is distributed in space (Figure 2g). To illustrate this sensitivity further, in Figure S2, we present additional simulations with spatial patterns of erosion and deposition that are as different as possible from those in Figure 1, and which, like Figure 2g, do not show strong correlations between the locations of sediment redistribution and the errors in ΔSL. These show that it is primarily the magnitude of the errors in ΔSL, rather than their spatial pattern, that is sensitive to the spatial patterns of erosion and deposition.

The magnitude of the errors in ΔSL is weakly sensitive to the spatial patterns of erosion and deposition because the amount of water incorporated into a sedimentary deposit depends on the geometry of the deposit. In the parameterization for compaction applied here, porosity decreases at a rate that scales with sediment thickness. If a given mass of sediment were deposited over a small area, it would be relatively thick and would compact quickly. Over a given time period, such a deposit would evolve toward a relatively small mean porosity and a relatively small volume of stored water. By contrast, if the same mass of sediment were deposited over a broad area, it would be relatively thin and would compact slowly, which would result in a relatively large mean porosity and a relatively large volume of stored water. This implies that the effects of sedimentary water storage on ΔSL should be sensitive to factors that influence the geometry of deposition, such as seafloor bathymetry and ocean currents (e.g., Gibbs, 1976; Storlazzi & Field, 2000), which highlights the need for accurate measurements and models of marine sediment transport and deposition.

As noted in section 2, in these simulations, we neglect any water stored in marine sedimentary pore space before the beginning of the model run. Including this effect will slightly reduce the net amount of water flowing into marine pore space due to water expulsion from underlying sediments that undergo compaction. The theory described here can incorporate this effect but would require detailed maps of global sediment thicknesses and estimates of their porosity to estimate its effects.

Temporal variations in sediment fluxes during a simulation should also influence the effects of sedimentary water storage, but only to the extent that they influence the mean porosity of the sediment deposits at the end of the simulation. Temporal variations in regional sediment fluxes during the last glacial period have been observed in a number of places over a range of timescales (Cartapanis et al., 2016; Dosseto et al., 2010; Goodbred & Kuehl, 2000a, 2000b; Herman et al., 2013; Herman & Champagnac, 2016; Hidy et al., 2014; Koppes et al., 2015; von Blanckenburg et al., 2015; Willenbring & Jerolmack, 2016), which suggests that the global sediment flux likely varied during the last glacial period, too. We are unaware of empirical constraints on temporal variations in the global sediment flux over the past glacial cycle, however, and therefore do not model the effects of such temporal variations here. Instead, we note that the model results in Figure 2 present motivation for obtaining stronger constraints the past history of global sediment fluxes.

A final implication of this analysis is that sedimentary water storage should continue increasing under continuous deposition. As long as deposition continues building larger deposits, the impact of sedimentary water storage on ΔSL should continue to increase. This implies that sedimentary water storage should be sensitive to changes in global rates of sediment delivery to the oceans. An illustrative case in point comes from surveys suggesting that terrigenous sedimentation rates were ~3.1 times faster during the most recent 5 Myr interval ($31.22 \cdot 10^{21}$ g) than during the previous 5 Myr interval ($10.15 \cdot 10^{21}$ g; Hay et al., 1988; Molnar, 2004). All else equal, this implies that roughly three times more water should have been introduced to terrigenous sedimentary pore space during 5–0 Ma than during 10–5 Ma. Even if the true temporal variations in sediment fluxes were smaller than this—for instance, if apparent deposition rates were biased by stochastic deposition or artifacts in sediment preservation (Sadler & Jerolmack, 2015; Willenbring & Jerolmack, 2016; Willenbring & von Blanckenburg, 2010)—the magnitude of the stored water sink implies that minor variations in global sediment fluxes can have significant effects on the global seawater budget over million-year timescales (e.g., Conrad, 2013; Miller et al., 2005).

5. Conclusions

The main contribution of this study is to demonstrate how the storage of water in marine sediment can affect modeled changes in sea level. To illustrate this, we used a gravitationally self-consistent sea-level model that has recently been extended to account for sedimentary water storage, and drove the model with a sediment redistribution history in which the rates and patterns of erosion and deposition are comparable to those at present and temporally steady over a glacial-interglacial cycle. Under this sediment redistribution scenario, modeled changes in sea level and global ice volume since the LIG would be in error by ~2 m GMSL if sediment redistribution were included but sedimentary water storage were neglected. Such an error would be significant in the context of published estimates of sea-level changes since the LIG (>6.6 m; Kopp et al., 2009; 6–9 m; Dutton & Lambeck, 2012). These simulations also demonstrate that the magnitude of global water fluxes into marine sediment are likely larger than the magnitude of water fluxes into and out of the ocean by volcanism and subduction. These results underscore the importance of accounting for sedimentary water storage in modeling sea-level changes over $>10^5$ year timescales.

Acknowledgments
K. L. F. and Q. L. were supported by NSF grant EAR-1525922, and T. P. was supported by an NSF Graduate Research Fellowship. J. A. acknowledges funding from the Royal Society. All data used are listed in the references, tables, and supporting information.

References

Austermann, J., & Mitrovica, J. X. (2015). Calculating gravitationally self-consistent sea level changes driven by dynamic topography. *Geophysical Journal International*, *203*(3), 1909–1922. https://doi.org/10.1093/gji/ggv371

Bahr, D. B., Hutton, E. W., Syvitski, J. P., & Pratson, L. F. (2001). Exponential approximations to compacted sediment porosity profiles. *Computers & Geosciences*, *27*(6), 691–700. https://doi.org/10.1016/S0098-3004(00)00140-0

Bebout, G. E. (1995). The impact of subduction-zone metamorphism on mantle-ocean chemical cycling. *Chemical Geology*, *126*(2), 191–218. https://doi.org/10.1016/0009-2541(95)00118-5

Bounama, C., Franck, S., & Von Bloh, W. (2001). The fate of Earth's ocean. *Hydrology and Earth System Sciences Discussions*, *5*(4), 569–576. https://doi.org/10.5194/hess-5-569-2001

Brain, M. J., Long, A. J., Woodroffe, S. A., Petley, D. N., Milledge, D. G., & Parnell, A. C. (2012). Modelling the effects of sediment compaction on salt marsh reconstructions of recent sea-level rise. *Earth and Planetary Science Letters*, *345*, 180–193.

Cartapanis, O., Bianchi, D., Jaccard, S. L., & Galbraith, E. D. (2016). Global pulses of organic carbon burial in deep-sea sediments during glacial maxima. *Nature Communications*, *7*, 10796. https://doi.org/10.1038/ncomms10796

Cathles, L. M. (1975). *The Viscosity of the Earth's Mantle*. Princeton, NJ: Princeton University Press.

Conrad, C. P. (2013). The solid Earth's influence on sea level. *Geological Society of America Bulletin*, *125*(7-8), 1027–1052. https://doi.org/10.1130/B30764.1

Dalca, A. V., Ferrier, K. L., Mitrovica, J. X., Perron, J. T., Milne, G. A., & Creveling, J. R. (2013). On postglacial sea level—III. Incorporating sediment redistribution. *Geophysical Journal International*, *194*(1), 45–60. https://doi.org/10.1093/gji/ggt089

Dosseto, A., Hesse, P. P., Maher, K., Fryirs, K., & Turner, S. (2010). Climatic and vegetation control on sediment dynamics during the last glacial cycle. *Geology*, *38*(5), 395–398. https://doi.org/10.1130/G30708.1

Dutton, A., & Lambeck, K. (2012). Ice volume and sea level during the last interglacial. *Science*, *337*(6091), 216–219. https://doi.org/10.1126/science.1205749

Dziewonski, A. M., & Anderson, D. L. (1981). Preliminary reference Earth model. *Physics of the Earth and Planetary Interiors*, *25*(4), 297–356. https://doi.org/10.1016/0031-9201(81)90046-7

Farrell, W. E., & Clark, J. A. (1976). On postglacial sea level. *Geophysical Journal International*, *46*(3), 647–667.

Ferrier, K. L., Austermann, J., Mitrovica, J. X., & Pico, T. (2017). Incorporating sediment compaction into a gravitationally self-consistent model for ice age sea-level change. *Geophysical Journal International*, *211*(1), 663–672. https://doi.org/10.1093/gji/ggx293

Ferrier, K. L., Mitrovica, J. X., Giosan, L., & Clift, P. D. (2015). Sea-level responses to erosion and deposition of sediment in the Indus River basin and the Arabian Sea. *Earth and Planetary Science Letters*, *416*, 12–20. https://doi.org/10.1016/j.epsl.2015.01.026

Fischer, T. P. (2008). Fluxes of volatiles (H_2O, CO_2, N_2, Cl, F) from arc volcanoes. *Geochemical Journal*, *42*(1), 21–38. https://doi.org/10.2343/geochemj.42.21

Gibbs, R. J. (1976). Amazon River sediment transport in the Atlantic Ocean. *Geology*, *4*(1), 45–48. https://doi.org/10.1130/0091-7613(1976)4%3C45:ARSTIT%3E2.0.CO;2

Global Runoff Data Centre (2007). *Major River basins of the world/global runoff data Centre*. Koblenz, Germany: Federal Institute of Hydrology (BfG).

Goldobin, D. S. (2011). Scaling of transport coefficients of porous media under compaction. *EPL (Europhysics Letters)*, *95*(6), 64004. https://doi.org/10.1209/0295-5075/95/64004

Goodbred, S. L., & Kuehl, S. A. (2000a). Enormous Ganges-Brahmaputra sediment discharge during strengthened early Holocene monsoon. *Geology*, *28*(12), 1083–1086. https://doi.org/10.1130/0091-7613(2000)28%3C1083:EGSDDS%3E2.0.CO;2

Goodbred, S. L., & Kuehl, S. A. (2000b). The significance of large sediment supply, active tectonism, and eustasy on margin sequence development: Late Quaternary stratigraphy and evolution of the Ganges–Brahmaputra delta. *Sedimentary Geology*, *133*(3-4), 227–248. https://doi.org/10.1016/S0037-0738(00)00041-5

Harrison, C. G. A. (1990). Long-term eustasy and epeirogeny in continents. In R. R. Revelle (Ed.), *Sea-level change* (pp. 141–158). Washington, DC: National Academy Press.

Harrison, C. G. A. (1999). Constraints on ocean volume change since the Archean. *Geophysical Research Letters*, *26*, 1913–1916. https://doi.org/10.1029/1999GL900425

Harrison, C. G. A., Brass, G. W., Saltzman, E., Sloan, J., Southam, J., & Whitman, J. M. (1981). Sea level variations, global sedimentation rates and the hypsographic curve. *Earth and Planetary Science Letters*, *54*(1), 1–16. https://doi.org/10.1016/0012-821X(81)90064-9

Hay, W. W., Sloan, J. L., & Wold, C. N. (1988). Mass/age distribution and composition of sediments on the ocean floor and the global rate of sediment subduction. *Journal of Geophysical Research*, *93*, 14,933–14,940. https://doi.org/10.1029/JB093iB12p14933

Herman, F., & Champagnac, J. D. (2016). Plio-Pleistocene increase of erosion rates in mountain belts in response to climate change. *Terra Nova*, *28*(1), 2–10. https://doi.org/10.1111/ter.12186

Herman, F., Seward, D., Valla, P. G., Carter, A., Kohn, B., Willett, S. D., & Ehlers, T. A. (2013). Worldwide acceleration of mountain erosion under a cooling climate. *Nature*, *504*(7480), 423–426. https://doi.org/10.1038/nature12877

Hidy, A. J., Gosse, J. C., Blum, M. D., & Gibling, M. R. (2014). Glacial–interglacial variation in denudation rates from interior Texas, USA, established with cosmogenic nuclides. *Earth and Planetary Science Letters*, *390*, 209–221. https://doi.org/10.1016/j.epsl.2014.01.011

Hilton, D. R., Fischer, T. P., & Marty, B. (2002). Noble gases in subduction zones and volatile recycling. *Reviews in Mineralogy and Geochemistry*, *47*(1), 319–370. https://doi.org/10.2138/rmg.2002.47.9

Ingebritsen, S. E., & Manning, C. E. (2002). Diffuse fluid flux through orogenic belts: Implications for the world ocean. *Proceedings of the National Academy of Sciences*, *99*(14), 9113–9116. https://doi.org/10.1073/pnas.132275699

Ito, E., Harris, D. M., & Anderson, A. T. (1983). Alteration of oceanic crust and geologic cycling of chlorine and water. *Geochimica et Cosmochimica Acta*, *47*(9), 1613–1624. https://doi.org/10.1016/0016-7037(83)90188-6

Jarrard, R. D. (2003). Subduction fluxes of water, carbon dioxide, chlorine, and potassium. *Geochemistry, Geophysics, Geosystems*, *4*(5), 8905. https://doi.org/10.1029/2002GC000392

Johnston, P. (1993). The effect of spatially non-uniform water loads on prediction of sea-level change. *Geophysical Journal International*, *114*(3), 615–634. https://doi.org/10.1111/j.1365-246X.1993.tb06992.x

Kirchner, J. W., & Ferrier, K. L. (2013). Earth science: Mainly in the plain. *Nature*, *495*(7441), 318–319. https://doi.org/10.1038/495318a

Kopp, R. E., Simons, F. J., Mitrovica, J. X., Maloof, A. C., & Oppenheimer, M. (2009). Probabilistic assessment of sea level during the last interglacial stage. *Nature*, *462*(7275), 863–867. https://doi.org/10.1038/nature08686

Kopp, R. E., Simons, F. J., Mitrovica, J. X., Maloof, A. C., & Oppenheimer, M. (2013). A probabilistic assessment of sea level variations within the last interglacial stage. *Geophysical Journal International*, *193*(2), 711–716. https://doi.org/10.1093/gji/ggt029

Koppes, M., Hallet, B., Rignot, E., Mouginot, J., Wellner, J. S., & Boldt, K. (2015). Observed latitudinal variations in erosion as a function of glacier dynamics. *Nature*, *526*(7571), 100–103. https://doi.org/10.1038/nature15385

Kuchar, J., Milne, G., Wolstencroft, M., Love, R., Tarasov, L., & Hijma, M. (2017). The influence of sediment isostatic adjustment on sea-level change and land motion along the US Gulf Coast. *Journal of Geophysical Research: Solid Earth*, *123*, 780–796. https://doi.org/10.1002/2017JB014695

Larsen, I. J., Montgomery, D. R., & Greenberg, H. M. (2014). The contribution of mountains to global denudation. *Geology*, *42*(6), 527–530. https://doi.org/10.1130/G35136.1

Latychev, K., Mitrovica, J. X., Tromp, J., Tamisiea, M. E., Komatitsch, D., & Christara, C. C. (2005). Glacial isostatic adjustment on 3-D Earth models: A finite-volume formulation. *Geophysical Journal International*, *161*(2), 421–444. https://doi.org/10.1111/j.1365-246X.2005.02536.x

Lehner B., Verdin K., & Jarvis A. (2006). *HydroSHEDS technical documentation*. World Wildlife Fund US, Washington, DC. Retrieved from http://hydrosheds.cr.usgs.gov

Martinec, Z. (2000). Spectral–finite element approach to three-dimensional viscoelastic relaxation in a spherical earth. *Geophysical Journal International*, *142*(1), 117–141. https://doi.org/10.1046/j.1365-246x.2000.00138.x

Miller, K. G., Kominz, M. A., Browning, J. V., Wright, J. D., Mountain, G. S., Katz, M. E., et al. (2005). The Phanerozoic record of global sea-level change. *Science*, *310*(5752), 1293–1298. https://doi.org/10.1126/science.1116412

Milliman, J. D., & Farnsworth, K. L. (2011). *Runoff, erosion, and delivery to the coastal ocean. River discharge to the coastal ocean: A global synthesis* (pp. 13–69). Cambridge, UK: Cambridge University Press.

Milne, G. A. (1998). Refining models of the glacial isostatic adjustment process. (PhD thesis) (pp. 1–123). University of Toronto.

Milne, G. A., & Mitrovica, J. X. (1996). Postglacial sea-level change on a rotating Earth: First results from a gravitationally self-consistent sea-level equation. *Geophysical Journal International*, *126*(3), F13–F20. https://doi.org/10.1111/j.1365-246X.1996.tb04691.x

Milne, G. A., & Mitrovica, J. X. (1998). Postglacial sea-level change on a rotating Earth. *Geophysical Journal International*, *133*(1), 1–19. https://doi.org/10.1046/j.1365-246X.1998.1331455.x

Milne, G. A., Mitrovica, J. X., & Davis, J. L. (1999). Near-field hydro-isostasy: The implementation of a revised sea-level equation. *Geophysical Journal International*, *139*(2), 464–482. https://doi.org/10.1046/j.1365-246x.1999.00971.x

Mitrovica, J. X., & Milne, G. A. (2002). On the origin of late Holocene sea-level highstands within equatorial ocean basins. *Quaternary Science Reviews*, *21*(20-22), 2179–2190. https://doi.org/10.1016/S0277-3791(02)00080-X

Molnar, P. (2004). Late Cenozoic increase in accumulation rates of terrestrial sediment: How might climate change have affected erosion rates? *Annual Review of Earth and Planetary Sciences*, *32*(1), 67–89. https://doi.org/10.1146/annurev.earth.32.091003.143456

Mondol, N. H., Bjørlykke, K., Jahren, J., & Høeg, K. (2007). Experimental mechanical compaction of clay mineral aggregates—Changes in physical properties of mudstones during burial. *Marine and Petroleum Geology*, *24*(5), 289–311. https://doi.org/10.1016/j.marpetgeo.2007.03.006

Moore, J. C., & Vrolijk, P. (1992). Fluids in accretionary prisms. *Reviews of Geophysics*, *30*, 113–135. https://doi.org/10.1029/92RG00201

Müller, R. D., Sdrolias, M., Gaina, C., Steinberger, B., & Heine, C. (2008). Long-term sea-level fluctuations driven by ocean basin dynamics. *Science*, *319*(5868), 1357–1362. https://doi.org/10.1126/science.1151540

Parai, R., & Mukhopadhyay, S. (2012). How large is the subducted water flux? New constraints on mantle regassing rates. *Earth and Planetary Science Letters*, *317*, 396–406.

Paulson, A., Zhong, S., & Wahr, J. (2007). Limitations on the inversion for mantle viscosity from postglacial rebound. *Geophysical Journal International*, *168*(3), 1195–1209. https://doi.org/10.1111/j.1365-246X.2006.03222.x

Peltier, W. R. (1994). Ice age paleotopography. *Science*, *265*(5169), 195–201. https://doi.org/10.1126/science.265.5169.195

Peltier, W. R. (2004). Global glacial isostasy and the surface of the ice-age Earth: The ICE-5G (VM2) model and GRACE. *Annual Review of Earth and Planetary Sciences*, *32*(1), 111–149. https://doi.org/10.1146/annurev.earth.32.082503.144359

Pico, T., Mitrovica, J. X., Ferrier, K. L., & Braun, J. (2016). Global ice volume during MIS 3 inferred from a sea-level analysis of sedimentary core records in the Yellow River Delta. *Quaternary Science Reviews*, *152*, 72–79. https://doi.org/10.1016/j.quascirev.2016.09.012

Revenga, C., Murray, S., Abramovitz, J., & Hammond, A. (1998). *Watersheds of the world: Ecological value and vulnerability*. Washington, DC: World Resources Institute.

Sadler, P. M., & Jerolmack, D. J. (2015). Scaling laws for aggradation, denudation and progradation rates: The case for time-scale invariance at sediment sources and sinks. *Geological Society, London, Special Publications*, *404*(1), 69–88. https://doi.org/10.1144/SP404.7

Screaton, E., Saffer, D., Henry, P., & Hunze, S. (2002). Porosity loss within the underthrust sediments of the Nankai accretionary complex: Implications for overpressures. *Geology*, *30*(1), 19–22. https://doi.org/10.1130/0091-7613(2002)030%3C0019:PLWTUS%3E2.0.CO;2

Shinohara, H. (2013). Volatile flux from subduction zone volcanoes: Insights from a detailed evaluation of the fluxes from volcanoes in Japan. *Journal of Volcanology and Geothermal Research*, *268*, 46–63. https://doi.org/10.1016/j.jvolgeores.2013.10.007

Southam, J. R., & Hay, W. W. (1977). Time scales and dynamic models of deep-sea sedimentation. *Journal of Geophysical Research*, *82*, 3825–3842. https://doi.org/10.1029/JC082i027p03825

Southam, J. R., & Hay, W. W. (1981). Global sedimentary mass balance and sea level changes. In C. Emiliani (Ed.), *The Sea* (Vol. 7, pp. 1617–1684). New York: Wiley.

Spinelli, G. A., Giambalvo, E. R., & Fisher, A. T. (2004). Sediment permeability, distribution, and influence on fluxes in oceanic basement. In E. E. Davis & H. Elderfied (Eds.), *Hydrogeology of the oceanic lithosphere* (pp. 151–188). Cambridge, UK: Cambridge University Press.

Spinelli, G. A., & Underwood, M. B. (2004). Character of sediments entering the Costa Rica subduction zone: Implications for partitioning of water along the plate interface. *Island Arc*, *13*(3), 432–451. https://doi.org/10.1111/j.1440-1738.2004.00436.x

Storlazzi, C. D., & Field, M. E. (2000). Sediment distribution and transport along a rocky, embayed coast: Monterey Peninsula and Carmel Bay, California. *Marine Geology*, *170*(3-4), 289–316. https://doi.org/10.1016/S0025-3227(00)00100-6

Syvitski, J. P., Vörösmarty, C. J., Kettner, A. J., & Green, P. (2005). Impact of humans on the flux of terrestrial sediment to the global coastal ocean. *Science*, *308*(5720), 376–380. https://doi.org/10.1126/science.1109454

United States Department of Commerce National Oceanic and Atmospheric Administration National Geophysical Data Center (2001). 2-Minute gridded global relief data (ETOPO2). Retrieved from http://www.ngdc.noaa.gov/mgg/fliers/01mgg04.html, Accessed 2006.

Veit, E., & Conrad, C. P. (2016). The impact of groundwater depletion on spatial variations in sea level change during the past century. *Geophysical Research Letters*, *43*, 3351–3359. https://doi.org/10.1002/2016GL068118

von Blanckenburg, F., Bouchez, J., Ibarra, D. E., & Maher, K. (2015). Stable runoff and weathering fluxes into the oceans over Quaternary climate cycles. *Nature Geoscience*, *8*(7), 538–542. https://doi.org/10.1038/ngeo2452

von Huene, R., & Scholl, D. W. (1991). Observations at convergent margins concerning sediment subduction, subduction erosion, and the growth of continental crust. *Reviews of Geophysics*, *29*, 279–316. https://doi.org/10.1029/91RG00969

Wada, Y., van Beek, L. P., van Kempen, C. M., Reckman, J. W., Vasak, S., & Bierkens, M. F. (2010). Global depletion of groundwater resources. *Geophysical Research Letters*, *37*, L20402. https://doi.org/10.1029/2010GL044571

Wallmann, K. (2001). The geological water cycle and the evolution of marine $\delta^{18}O$ values. *Geochimica et Cosmochimica Acta*, *65*(15), 2469–2485. https://doi.org/10.1016/S0016-7037(01)00603-2

Wilkinson, B. H., & McElroy, B. J. (2007). The impact of humans on continental erosion and sedimentation. *Geological Society of America Bulletin*, *119*(1-2), 140–156. https://doi.org/10.1130/B25899.1

Willenbring, J. K., Codilean, A. T., & McElroy, B. (2013). Earth is (mostly) flat: Apportionment of the flux of continental sediment over millennial time scales. *Geology*, *41*(3), 343–346. https://doi.org/10.1130/G33918.1

Willenbring, J. K., & Jerolmack, D. J. (2016). The null hypothesis: Globally steady rates of erosion, weathering fluxes and shelf sediment accumulation during Late Cenozoic mountain uplift and glaciation. *Terra Nova*, *28*(1), 11–18. https://doi.org/10.1111/ter.12185

Willenbring, J. K., & von Blanckenburg, F. (2010). Long-term stability of global erosion rates and weathering during late-Cenozoic cooling. *Nature*, *465*(7295), 211–214. https://doi.org/10.1038/nature09044

Wolstencroft, M., Shen, Z., Törnqvist, T. E., Milne, G. A., & Kulp, M. (2014). Understanding subsidence in the Mississippi Delta region due to sediment, ice, and ocean loading: Insights from geophysical modeling. *Journal of Geophysical Research: Solid Earth*, *119*, 3838–3856. https://doi.org/10.1002/2013JB010928

Woodruff, J. D., Irish, J. L., & Camargo, S. J. (2013). Coastal flooding by tropical cyclones and sea-level rise. *Nature*, *504*(7478), 44–52. https://doi.org/10.1038/nature12855

Wu, P., & van der Wal, W. (2003). Postglacial sealevels on a spherical, self-gravitating viscoelastic earth: Effects of lateral viscosity variations in the upper mantle on the inference of viscosity contrasts in the lower mantle. *Earth and Planetary Science Letters*, *211*(1-2), 57–68. https://doi.org/10.1016/S0012-821X(03)00199-7

Zhong, S., Paulson, A., & Wahr, J. (2003). Three-dimensional finite-element modelling of Earth's viscoelastic deformation: Effects of lateral variations in lithospheric thickness. *Geophysical Journal International*, *155*(2), 679–695. https://doi.org/10.1046/j.1365-246X.2003.02084.x